

## Grape seed extract induces apoptotic death of human prostate carcinoma DU145 cells via caspases activation accompanied by dissipation of mitochondrial membrane potential and cytochrome *c* release

Chapla Agarwal<sup>1,3</sup>, Rana P.Singh<sup>1</sup> and Rajesh Agarwal<sup>1,2</sup>

<sup>1</sup>Department of Pharmaceutical Sciences, School of Pharmacy, University of Colorado Health Sciences Center, Denver, CO 80262, and <sup>2</sup>University of Colorado Cancer Center, University of Colorado Health Sciences Center, Denver, CO 80262, USA

<sup>3</sup>To whom correspondence should be addressed at: Department of Pharmaceutical Sciences, School of Pharmacy, University of Colorado Health Sciences Center, 4200 East Ninth Street, Box C238, Denver, CO 80262, USA  
Email: Chapla.Agarwal@UCHSC.edu

**Grape seed extract (GSE), rich in the bioflavonoids commonly known as procyanidins, is one of the most commonly consumed dietary supplements in the United States because of its several health benefits. Epidemiological studies show that many prostate cancer (PCA) patients use herbal extracts as dietary supplements in addition to their prescription drugs. Accordingly, in recent years, we have focused our attention on assessing the efficacy of GSE against PCA. Our studies showed that GSE inhibits growth and induces apoptotic death of human PCA cells in culture and in nude mice. Here, we performed detailed studies to define the molecular mechanism of GSE-induced apoptosis in advanced human PCA DU145 cells. GSE treatment of cells at various doses (50–200 µg/ml) for 12–72 h resulted in a moderate to strong apoptotic death in a dose- and time-dependent manner. In the studies assessing the apoptotic-signaling pathway induced by GSE, we observed an increase in cleaved fragments of caspases 3, 7 and 9 as well as PARP in GSE-treated cells after 48 and 72 h of treatment. Pre-treatment of cells with general caspases inhibitor, z-Val-Ala-Asp(OMe)-FMK or caspase 3-like proteases inhibitor [z-Asp(OMe)-Glu(OMe)-Val-Asp(OMe)-FMK], almost completely (~90%) inhibited the GSE-induced apoptotic cell death. In a later case, GSE-induced caspase-3 activity was completely inhibited. Selective caspase 9 inhibitor [z-Leu-Glu(OMe)-His-Asp(OMe)-FMK] showed only partial inhibition of GSE-induced apoptosis whereas GSE-induced protease activity of caspase 9 was completely inhibited. Upstream of caspase cascade, GSE showed disappearance of mitochondrial membrane potential and an increase in cytochrome *c* release in cytosol. Together, these results suggest that GSE possibly causes mitochondrial damage leading to cytochrome *c* release in cytosol and activation of caspases resulting in PARP cleavage and execution of apoptotic death of human PCA DU145 cells. Furthermore, GSE-caused caspase 3-mediated apoptosis also involves other pathway(s) including caspase 9 activation.**

**Abbreviations:** DEVD, Asp-Glu-Val-Asp;  $\Delta\psi_m$ , mitochondrial membrane potential, FACS, fluorescence activated cell sorting; FMK, fluoromethylketone; PCA, prostate cancer; GSE, grape seed extract; LEHD, Leu-Glu-His-Asp; PARP, poly (ADP-ribose) polymerase; PI, propidium iodide; *p*NA, *p*-nitroanilide; z, benzyloxycarbonyl; VAD, Val-Ala-Asp.

### Introduction

Prostate cancer (PCA) is the most invasive and frequently diagnosed malignancy, and the second leading cause of cancer-related deaths in the United States males (1). Each year about half of the diagnosed PCA patients eventually develop incurable disease with no effective treatment option left for them (1). The autocrine and paracrine growth factor-receptor interactions and associated mitogenic signaling as well as defects in apoptotic signaling are the major contributors in unchecked proliferation and immortalization of PCA cells (2,3). In the advanced stage, PCA growth and development become independent of androgen and renders androgen ablation therapy ineffective, as cancer cells develop resistant to androgen withdrawal associated apoptosis (4). The development of resistance against apoptosis in advanced PCA cells makes chemotherapeutic agents almost ineffective in treating the disease (5). Accordingly, developing new therapeutic strategies targeted at apoptosis induction could be effective in controlling the proliferation as well as invasiveness of advanced stages of PCA. In this respect, the evaluation of anticancer effects of various natural (plant-derived) agents has gained widespread attention in recent years with the hope that a positive outcome from such studies could provide a scientific basis for their efficacy and usefulness in chemoprevention/chemotherapy of several cancers including PCA (3,6,7).

Grape seed extract (GSE) is a natural rich source of the bioflavonoids commonly known as procyanidins. Commercial preparations of GSE, widely referred to as 'Grape Seed Extract standardized to contain 95% oligomeric procyanidins', are marketed in the United States as a dietary supplement offering several health benefits (8). Epidemiological studies suggest that diet composition plays an important role in cancer risk management (6). In general, one in every five individuals takes herbal extracts as dietary supplement, and as many PCA patients consume dietary supplements in addition to prescription drugs; overall the therapies based on alternative or complementary medicines are becoming increasingly popular among PCA patients (9).

In addition to several other health-related benefits, GSE has been shown to exert anticancer effects against various human carcinoma cells in culture, including PCA (10–12). For example, in recent studies, we showed that GSE strongly inhibits the growth of human prostate carcinoma DU145 cells accompanied with apoptotic cell death in culture (10) and in nude mice (Singh *et al.*, manuscript under review).

There are some reports suggesting that GSE could be a potential cancer chemopreventive agent against various epithelial cancers in animal studies (13,14). However, detailed studies have not been performed yet to develop GSE as a mechanism-based anticancer agent. Here, we investigated the molecular mechanisms of GSE-caused apoptotic death of human PCA DU145 cells.

## Materials and methods

### Cell line and reagents

Human prostate carcinoma cell line DU145 was obtained from American Type Culture Collection (Manassas, VA). Cells were cultured in RPMI 1640 with 10% fetal bovine serum (Hyclone) under standard culture conditions (37°C, 95% humidified air and 5% CO<sub>2</sub>). RPMI 1640 and other culture materials were from Life Technologies (Gaithersburg, MD). GSE used in the present study was from Traco Labs (Champaign, IL). We would like to mention here that to avoid batch-to-batch and/or lot-to-lot variation in GSE preparation and to maintain consistency in our studies, we have obtained a large quantity of one batch/lot of GSE from Traco Labs that is being used in all our studies (10). All caspases and poly (ADP-ribose) polymerase (PARP) primary antibodies, and peroxidase-conjugated secondary antibody were from Cell Signaling Technology (Beverly, MA). Caspase inhibitors were from Enzyme Systems Products (Livermore, CA). Annexin V/propidium iodide (PI) and JC-1 staining kits were from Molecular Probes (Eugene, OR). ECL detection system was from Amersham Corp. (Arlington Heights, IL). Other chemicals were obtained in their commercially available highest purity grade.

### Quantitative apoptotic cell death assay

To quantify GSE-induced apoptotic death of DU145 cells, annexin V and PI staining was performed followed by flow cytometry, as described recently (10). Briefly, after treatment of cells with GSE and/or different caspase inhibitors at desired doses and time-points, both floating and attached cells were collected by brief trypsinization and washed with PBS twice, then subjected to annexin V and PI staining using Vybrant Apoptosis Assay Kit2 (Molecular Probes, Eugene, OR) following the step-by-step protocol provided by the manufacturer. The kit contains recombinant annexin V conjugated to fluorophores and the Alexa fluoro 488 dye, providing maximum sensitivity. After staining, flow cytometry was performed for the quantification of apoptotic cells.

### Immunoblot analysis

Following GSE treatments, cell lysates were prepared in non-denaturing lysis buffer (10 mM Tris-HCl, pH 7.4, 150 mM NaCl, 1% Triton X-100, 1 mM EDTA, 1 mM EGTA, 0.3 mM phenyl methyl sulfonyl fluoride, 0.2 mM sodium orthovanadate, 0.5% NP-40, 5 U/ml aprotinin). For lysate preparation, medium was aspirated and cells were washed twice with ice-cold PBS followed by incubation in non-denaturing lysis buffer for 20 min. Then, cells were scrapped and kept on ice for an additional 30 min, and finally cell lysates were cleared by centrifugation at 4°C for 30 min in a tabletop centrifuge. Protein concentration in lysates was determined using Bio-Rad DC protein assay kit (Bio-Rad laboratories, Hercules, CA) by the Lowry method. For immunoblot analyses, 70–100 µg of protein lysates per sample were denatured in 2× SDS-PAGE sample buffer and subjected to SDS-PAGE on 8, 12 or 16% Tris-glycine gel as needed. The separated proteins were transferred onto nitrocellulose membrane followed by blocking with 5% non-fat milk powder (w/v) in TBS (10 mM Tris, 100 mM NaCl, 0.1% Tween 20) for 1 h at room temperature or overnight at 4°C. Membranes were probed for the protein levels of cleaved caspases 9, 7 and 3, as well as PARP and β-actin using specific primary antibodies followed by peroxidase-conjugated appropriate secondary antibody, and visualized by ECL detection system.

### Cytometric bead array analysis for active caspase 3

BD Human Active Caspase 3 CBA Kit (BD Biosciences, San Diego, CA) was used to quantify active caspase 3 levels following manufacturer's protocol. The principle of the assay was based on detection of a single bead population with a distinct fluorescence intensity coated with capture antibody specific for human active caspase 3 protein (15). At the end of assay procedure, sandwich complexes were resolved in FL3 channel of flow cytometer followed by acquisition of sample data. BD CBA analysis software was used to analyze the data. Finally, caspase 3 was quantified (pg/ml cell lysate) using 4-parameter logistic curve-fit model generated standard curve from 'human active caspase 3 lysate standard' supplied with the kit. Flow cytometry and data analysis were done by the FACS core facility of University of Colorado Cancer Center.

### Caspase activity assay

Caspase 3-like (caspases 3 and 7) and caspase 9 activities were assayed by the colorimetric protease assay ApoTarget kit (BioSource International, CA) following manufacturer's protocol. Briefly, at the end of treatment with either 150 µg/ml dose of GSE or caspases inhibitors (100 µM) or both (150 µg/ml dose of GSE and 25, 50 and 100 µM caspases inhibitors) for 72 h, cells were collected and cell lysates prepared in cell lysis buffer (Tris-buffered saline containing detergent). 200 µg of protein lysate per sample was mixed with 2× reaction buffer and 200 µM substrate (DEVD-pNA for caspase 3-like and LEHD-pNA for caspase 9), and incubated at 37°C for 2 h in the dark. These assay conditions are standardized and products of the reaction

remain in the linear range of detection. Developed color was measured at 405 nm in a microplate reader, and blank reading was subtracted from each sample reading before calculation.

### Mitochondrial membrane potential ( $\Delta y_m$ ) analysis

Alterations in  $\Delta y_m$  were analyzed by flow cytometry using the mitochondrial membrane potential sensitive cationic dye JC-1 and following the vendor's protocol with some modification. Briefly, cells were treated with 150 and 200 µg/ml doses of GSE for desired durations, and at the end of treatment, adherent cells were washed with PBS and harvested by a brief trypsinization followed by another wash with PBS. Cells were incubated with JC-1 (10 µg/ml in PBS) at 37°C for 10 min. Stained cells were washed with PBS twice and analyzed by flow cytometry. A minimum of 10 000 cells/sample were analyzed by Becton Dickinson FACScan System at flow cytometry core facility of University of Colorado Cancer Center. Valinomycin was used as positive control. Forward scatter versus side scatter was used to gate the viable population of cells. JC-1 exhibits potential-dependent accumulation in mitochondria, indicated by a fluorescence emission shift from green to red. The emission wavelengths of JC-1 monomers and 'J-aggregates' were ~525 (FL-1 channel) and ~590 (FL-2 channel) nm. JC-1 is most widely applied for detecting mitochondrial depolarization occurring in the early stages of apoptosis (16).

### Preparation of cytosolic extract and immunoblot analysis of cytochrome c release

At the end of GSE treatment, cells were washed with ice-cold PBS and collected by a brief trypsinization followed by two more washes with PBS. The cell pellet was resuspended in 200 µl of extraction buffer containing 210 mM mannitol, 70 mM sucrose, 20 mM HEPES-KOH, pH 7.4, 50 mM KCl, 5 mM EGTA, 2 mM MgCl<sub>2</sub>, 1 mM dithiothreitol, 0.1 mM PMSF and protease inhibitors (Complete Cocktail; Roche Molecular Biochemicals, Indianapolis, IN). After 20 min incubation on ice, cells were homogenized with a glass Dounce and pestle, and resulting homogenates were left on ice for an additional 20 min. Homogenates were centrifuged at 10 000 g for 15 min at 4°C, and resulting supernatant was further centrifuged at 18 000 g for 30 min at 4°C, to yield cytosolic extract. 70 µg protein per sample was resolved on 16% SDS-PAGE and transferred onto nitrocellulose membrane followed by blocking in 5% (w/v) non-fat dry milk in TBS. Membrane was probed with anti-cytochrome c antibody (BD PharMingen, San Diego, CA) overnight at 4°C followed by 1 h incubation with HRP-conjugated secondary antibody. The protein was visualized using the ECL detection system.

### Immunohistochemical sub-cellular localization of cytochrome c

DU145 cells were seeded on four-well chamber slides and next day treated with either DMSO (control) or 150 µg/ml GSE dissolved in DMSO for 12 h. At the end of the treatment, cells were fixed with methanol at -20°C for 10 min and washed twice with ice-cold PBS. Cells were gradually rehydrated with PBS and then incubated with 10% BSA in PBS for 30 min at room temperature. Cells were rinsed twice with PBS and incubated with primary mouse anti-cytochrome c monoclonal antibody (PharMingen, San Diego, CA) in PBS with 3% BSA at 4°C overnight. Cells were then rinsed in PBS with 3% BSA six times and incubated with goat Alexa 488-conjugated anti-mouse IgG secondary antibody (Molecular Probes, Eugene, OR) in PBS with 3% BSA for 1 h. Cells were then rinsed in PBS with 3% BSA six times and observed and photographed under inverted Nikon TE-300 microscope with an epifluorescent attachment equipped with a Princeton Instrument Micromax camera, at 488 nm fluorescence excitation and 520 nm fluorescence emission. Images are acquired with Image Pro-plus software (Media Cybernetics, Silver Spring, MD).

### Statistical analysis

The data were analyzed using the Jandel Scientific SigmaStat 2.0 software. Student's *t*-test was employed to assess the statistical significance of the difference between control and different treatment groups. A statistically significant difference was considered to be present at *P* < 0.05.

## Results

### GSE induces dose- and time-dependent apoptosis in DU145 cells

First we assessed dose- (50–200 µg/ml) and time-dependent (24–96 h) apoptotic death effect of GSE in DU145 cells using annexin V and PI staining. As shown in Figure 1, GSE induced a moderate to strong apoptotic death in both dose- and time-dependent manner. In initial dose-response study, GSE treatment for 48 h at 50–200 µg/ml doses resulted in

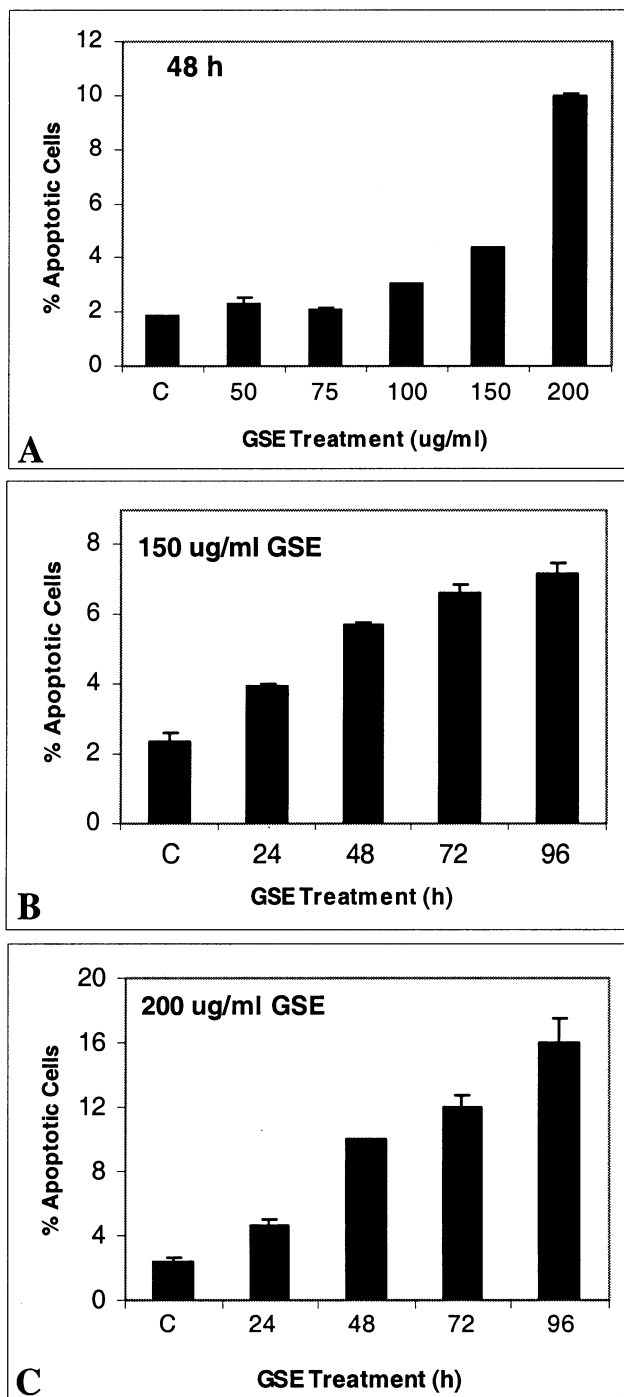


**Fig. 1.** Dose and time course of GSE-induced apoptotic cell death in DU145 cells. Cells were plated in 60 mm dishes, and were fed with fresh medium either with vehicle (DMSO, 0.1% final concentration) alone or 50–200 µg/ml doses of GSE. After 12, 24, 48 and 72 h of these treatments, cells were harvested and stained with annexin V/PI and analyzed by flow cytometry. Apoptotic effects of GSE: (A) dose-dependent at 48 h; (B) 150 µg/ml and (C) 200 µg/ml GSE doses for time-points. Data are presented as mean  $\pm$  SE of percent annexin V/PI stained cells of two independent samples in each treatment group.

2.3–10.0% apoptotic cell death in dose-dependent manner compared with control showing 1.8% apoptotic cells (Figure 1A). In a time-response study, 150 and 200 µg/ml doses of GSE for 24–96 h resulted in 4.0–7.2% and 4.6–16.0% apoptotic cell death, respectively, compared with that of control showing 2.4% apoptotic cell death (Figure 1B and C).

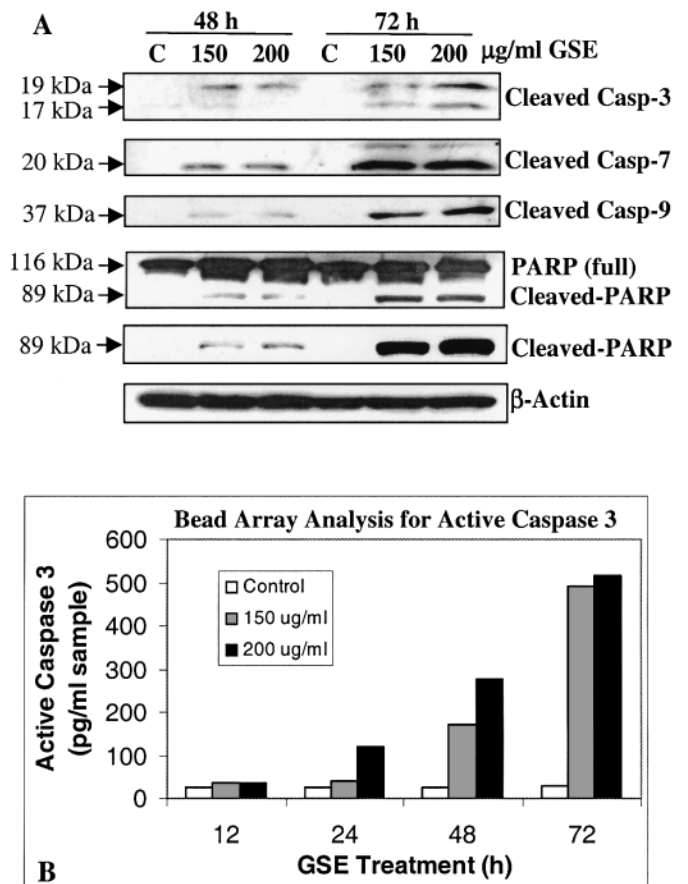


**Fig. 2.** Effect of GSE on the cleavage patterns of caspase 3, 7 and 9, and PARP in DU145 cells. (A) Cells were grown at standard culture conditions as mentioned in Materials and methods, and treated with 150 and 200 µg/ml doses of GSE for 48–72 h, and cell lysates were prepared. Immunoblot analysis was performed to identify the cleaved products of caspase 3, caspase 7 and caspase 9, and full and cleaved PARP using specific primary antibodies. Loading was checked by immunoblotting of  $\beta$ -actin. Bands were visualized by ECL detection system. Data shown are representative of three independent experiments. (B) Cells were grown at standard culture conditions as mentioned in Materials and methods, and treated with 150 and 200 µg/ml doses of GSE for 12–72 h, and cell lysates were prepared following cytometric bead array vendor manual. Beads containing active human caspase 3 were resolved in FL3 channel of flow cytometer followed by acquisition of sample data. BD CBA analysis software was used to analyze the data. Active caspase 3 was quantified using 4-parameter logistic curve-fit model generated standard curve from 'human active caspase 3 lysate standard' supplied with the kit, and presented as pg/ml cell lysate. Casp, caspase.

#### GSE causes caspases and PARP cleavage in DU145 cells

Based on increased apoptosis in GSE-treated cells, our next aim was to examine the involvement of caspases that play a major role in execution of apoptotic events. Accordingly, first we investigated the levels of cleaved active sub-units of pro-caspases (inactive) by immunoblot analysis in cell lysates. Treatment of cells with 150 and 200 µg/ml doses of GSE for 48 and 72 h showed a prominent increase in the cleaved sub-units of caspase 3 (17 and 19 kDa), caspase 7 (20 kDa) and caspase 9 (37 kDa) (Figure 2A). At similar GSE doses we could not observe the detectable levels of these cleaved caspases (data not shown). The effect of GSE on the protein levels of cleaved caspases that directly corresponds with their cysteine protease activity appears to be time-dependent at investigated doses (Figure 2A). Since PARP is one the downstream substrates of caspase cascade and an excellent marker

of apoptosis, next we examined the effect of GSE-caused caspases activation on PARP cleavage which separates *N*-terminal DNA-binding domain from its *C*-terminal catalytic domain (89 kDa) (17). Our immunoblot analysis showed the detectable level of cleaved PARP (89 kDa) at 48 and 72 h of GSE treatment (Figure 2A) that corresponds to and further supports the possible involvement of caspases activation in GSE-caused apoptosis in DU145 cells. Membranes were probed with  $\beta$ -actin for loading correction, which did not show any marked change in the protein level of  $\beta$ -actin (Figure 2A).

Furthermore, we performed cytometric bead array analysis for active caspase 3 protein level which is the major executioner caspase in the caspase cascade. This method is more sensitive, specific and precise when compared with western immunoblotting. The result of this study showed that GSE has a very strong and dose- as well as time-dependent effect on the induction of active caspase 3 level. Even 12 h of GSE (150 and 200  $\mu\text{g/ml}$ ) treatment increased the active caspase 3 level by 1.5 fold (Figure 2B). These treatments for 24 h resulted in 1.6–4.7 fold increase in the active caspase 3 level, however due to sensitivity limit we could detect these protein levels in western immunoblotting after 12 and 24 h of treatment. At later time points, 48 and 72 h, similar GSE treatment resulted in 7.1–11.5 and 16.5–17.4 fold increase in active caspase 3 level, respectively (Figure 2B). At higher time points both GSE doses seems to have almost similar effects which was also evident in western immunoblotting for cleaved caspase 3.

*GSE-induced apoptosis is largely mediated via caspases activation*

To further establish the involvement of caspases in GSE-induced apoptosis in DU145 cells, we employed a pharmacological inhibitor approach using a general as well as specific caspases inhibitors either alone or in combination with GSE followed by annexin V/PI staining and FACS analysis. Treatment with caspases inhibitors (100  $\mu\text{M}$ ) showed either slightly lower or comparable apoptotic cell death with that of control (Figure 3). Co-treatment of cells with GSE (150  $\mu\text{g/ml}$ ) and different doses of a general caspase inhibitor z-VAD-fmk (25, 50 and 100  $\mu\text{M}$ ) for 72 h strongly inhibited the GSE-induced apoptosis (Figure 3A). Both lower doses of the inhibitor showed almost similar effect (~75% inhibition) whereas the 100  $\mu\text{M}$  dose caused 90% inhibition in GSE-induced apoptosis. Next, we investigated the involvement of specific caspases namely, caspase 9 and 3-like (caspase 3 and 7). Co-treatment of cells with GSE (150  $\mu\text{g/ml}$ ) and different doses of caspase 9 inhibitor z-LEHD-fmk (25, 50 and 100  $\mu\text{M}$ ), did not completely inhibit the GSE-induced apoptosis (Figure 3B). The magnitude of inhibitory effect was almost similar at all the three doses of the inhibitor accounting for 35–45% inhibition of GSE-caused apoptosis. When cells were co-treated with GSE (150  $\mu\text{g/ml}$ ) and different doses of caspase 3-like inhibitor z-DEVD-fmk (25, 50 and 100  $\mu\text{M}$ ) a strong inhibition in GSE-induced apoptosis was observed, which accounted for 82–91% inhibition (Figure 3C) and was comparable with the inhibitory effect of general caspases inhibitor. Together, these results indicated that GSE-induced apoptosis in DU145 cells is largely mediated via activation of caspase pathway. However, caspase 9 inhibitor could neither completely block nor showed similar inhibitory effect on GSE-induced apoptosis compared with caspase 3 inhibitor. Therefore, GSE-caused activation of caspase 9 could have a partial role in the activation of caspase 3. These results also suggest that additional mechanism(s)

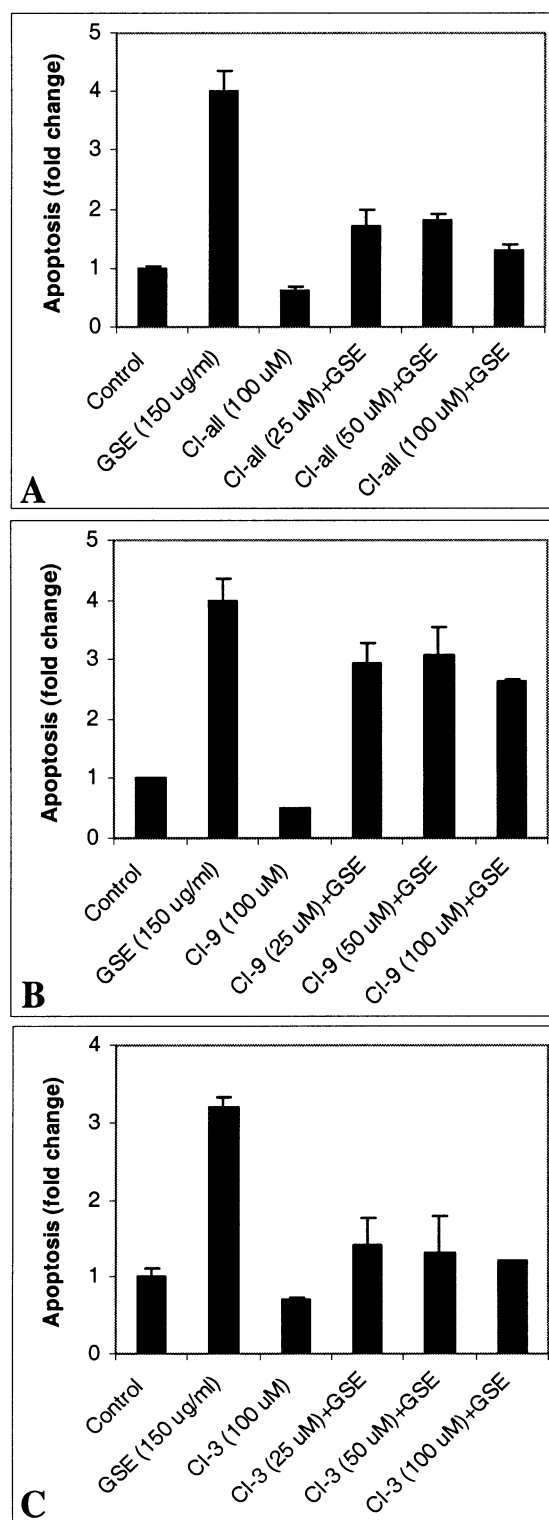


**Fig. 3.** Effect of caspases inhibitors on GSE-induced apoptosis in DU145 cells. Cells were grown in similar condition as in Figure 2, and treated with either vehicle (DMSO) control or GSE (150  $\mu\text{g/ml}$ ) or caspases inhibitors; z-VAD-fmk (a general caspase inhibitor), z-LEHD-fmk (caspase 9 inhibitor) and z-DEVD-fmk (caspase 3-like inhibitor) alone (100  $\mu\text{M}$ ) or in combination (25, 50 and 100  $\mu\text{M}$ ) with GSE. After 72 h of these treatments, cells were harvested and analyzed for apoptosis by annexin V/PI staining followed by FACS analysis. Data are presented as mean  $\pm$  SE of percent annexin V/PI stained cells of two–three independent samples in each treatment group. Experiment was repeated with similar results.

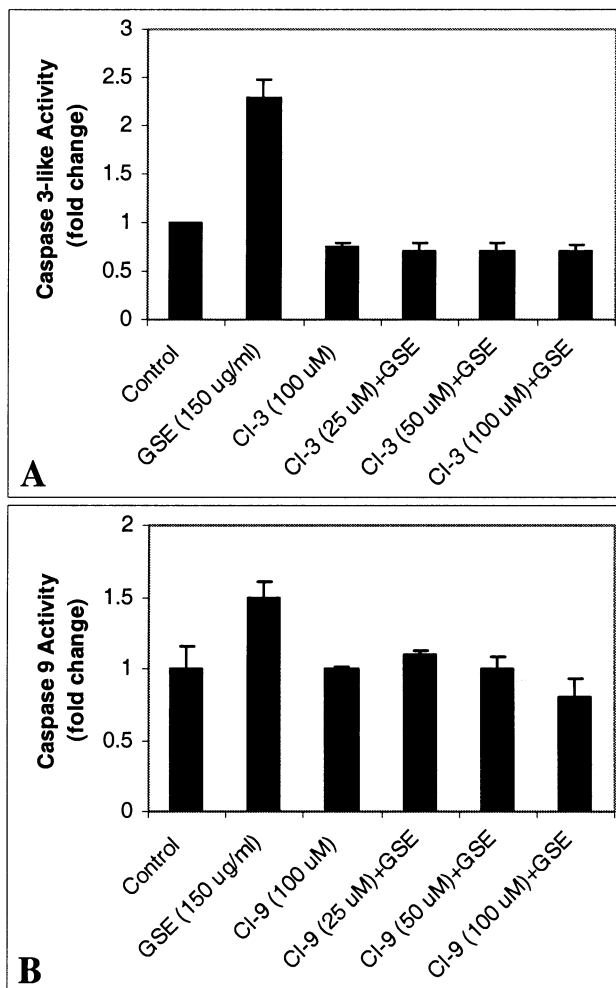


**Fig. 4.** Effect of GSE and caspase inhibitors on the activity of caspase-3-like and caspase 9. Cells were grown in similar condition as in Figure 2, and treated with either vehicle (DMSO) control or GSE (150 µg/ml) or caspases inhibitors; z-LEHD-fmk (caspase 9 inhibitor) and z-DEVD-fmk (caspase 3 inhibitor) alone (100 µM) or in combination (25, 50 and 100 µM) with GSE. After 72 h of these treatments, cells were harvested and cell lysates prepared. The enzymatic activity of cell lysates towards tetrapeptide substrates, (A) DEVD-pNA (for caspase 3-like) and (B) LEHD-pNA (for caspase 9) was determined. Caspase activities are expressed as fold change of control and presented as mean  $\pm$  SE of two samples. Experiment was repeated with similar results. CI-3, caspase 3-like (caspase 3 and 7) inhibitor; CI-9, caspase 9 inhibitor.

might be involved in GSE-caused apoptotic death of DU145 cells mediated via caspase 3 activation which is yet to be investigated.

Furthermore, to support these findings we checked whether the doses of caspase 9 and 3-like inhibitors used in the study were sufficient to block the protease activity of these caspases. We analyzed the enzyme activities against tetrapeptide substrates linked with chromophore *p*-nitroanilide; DEVD*p*-NA for caspase 3-like (caspase 3 and 7) and LEHD*p*-NA for caspase 9. The hydrolytic enzyme activity of caspase 3-like caspases towards DEVD*p*-NA was elevated by 2.3 fold at 150 µg/ml dose of GSE treatment for 72 h (Figure 4A). The GSE-induced caspase 3-like activity was completely abolished when cells were co-treated with GSE and the specific inhibitor (at all doses) (Figure 4A). Similarly, GSE-induced caspase 9 activity was also abolished by the use of the specific inhibitor (Figure 4B). These results convincingly supported the above

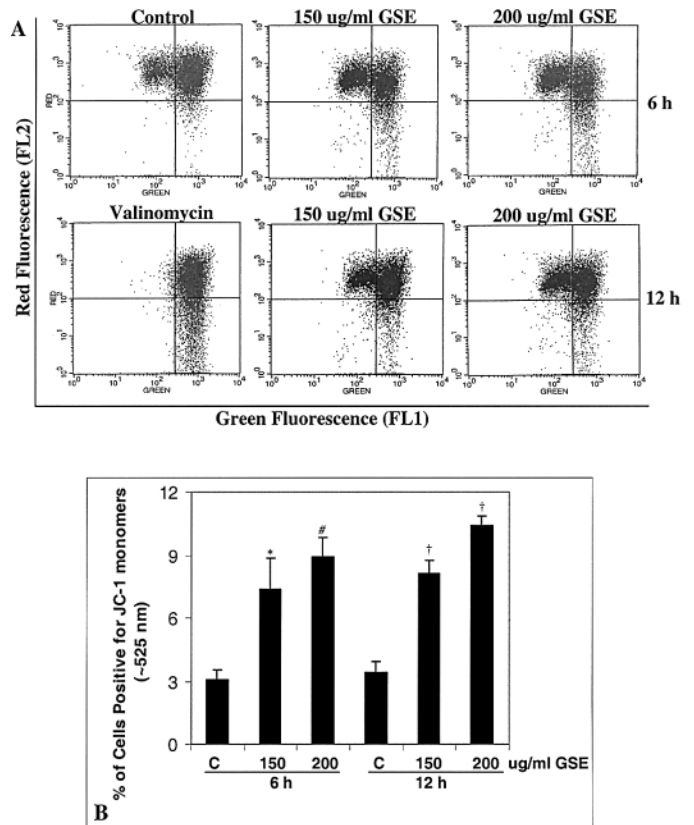


**Fig. 5.** JC-1 Staining for GSE-induced dissipation of mitochondrial membrane potential in DU145 cells. Cells were treated with 150 and 200 µg/ml doses of GSE for 6 and 12 h, and stained with JC-1 (10 µg/ml in PBS), a mitochondrial potential sensitive dye, and a minimum of 10 000 cells/sample were analyzed by flow cytometry. (A) Fluorescence pattern of different treatment groups as indicated in the figure; valinomycin was used as positive control and gating correction, (B) quantitative presentation of the data as (mean  $\pm$  SE of three samples) percent of positive JC-1 stained cells. Forward scatter vs. side scatter was used to gate the viable population of cells. The emission wavelengths of JC-1 monomers and 'J-aggregates' were ~527 (FL-1 channel) and ~590 (FL-2 channel) nm. Data presented are representative of two independent experiments. \*,  $P < 0.05$ ; #,  $P < 0.01$  and †,  $P < 0.001$  versus control.

hypothesis and also suggested that a small fraction of GSE-caused apoptosis might be mediated via other pathway(s) besides caspase cascade activation.

#### GSE disrupts mitochondrial membrane potential in DU145 cells

Mitochondrial integrity or the loss of  $\Delta\psi_m$  has been linked to the initiation and activation of some apoptotic cascades (18,19). To determine whether GSE-induced apoptosis in DU145 cells involves mitochondrial disruption, we examined the depolarization of mitochondrial membrane by measuring the fluorescence emission shift (red to green) of the  $\Delta\psi_m$  sensitive cationic JC-1 dye. DU145 cells were treated with 150 and 200 µg/ml doses of GSE for 6 and 12 h, and at the end of treatments, cells were processed and stained with JC-1 dye and analyzed by flow cytometry. GSE treatment of cells showed an increase in green/red fluorescence intensity indicative of mitochondrial membrane depolarization as depicted by cytofluorimetric analysis (Figure 5A). Quantification of JC-1 monomer positive cells (right lower rectangle) showed a significant dose-dependent increase following GSE treatment accounting for 7.4–8.9% ( $P < 0.05$ –0.01) and 8.1–10.4% ( $P < 0.01$ –0.001) positive cells at 6 and 12 h of GSE treatments, respectively,

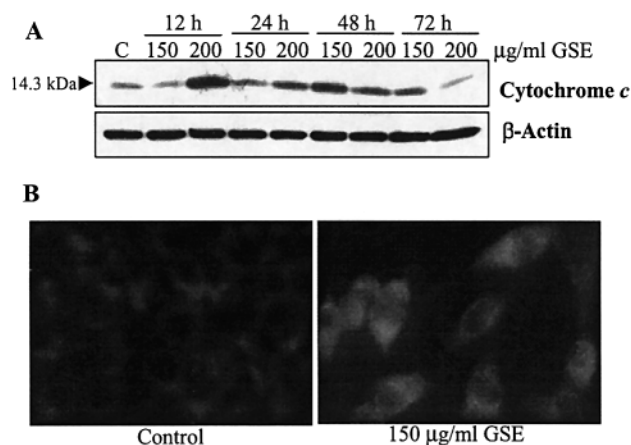


**Fig. 6.** Effect of GSE on cytochrome *c* release from mitochondria to the cytoplasm. (A) Western immunoblot analysis where DU145 cells were treated with 150 and 200  $\mu$ g/ml doses of GSE for 12–72 h, and then cells were harvested and cytosolic extracts were prepared as described in Materials and methods. 70  $\mu$ g protein per sample was resolved on 16% SDS–PAGE and transferred onto nitrocellulose membrane followed by blocking in 5% non-fat dry milk. Membrane was probed with anti-cytochrome *c* antibody followed by incubation with peroxidase-conjugated secondary antibody. The protein was visualized by ECL detection system. Same membrane was blotted for  $\beta$ -actin (bottom panel) for loading correction. Data shown are representative of three independent experiments. (B) Immunohistochemical analysis of GSE-induced cytochrome *c* release from mitochondria to the cytosol. DU145 cells were treated with vehicle (DMSO) alone or 150  $\mu$ g/ml dose of GSE for 12 h followed by intracellular cytochrome *c* staining as detailed in Materials and methods. A less intense and less diffuse staining pattern of intracellular cytochrome *c* in control cells indicates its localization mostly within mitochondria, whereas a more intense and marked diffuse staining pattern after GSE treatment indicating that cytochrome *c* is released from some mitochondria into the cytosol. Microscopic images are taken under inverted Nikon TE-300 microscope with an epifluorescent attachment equipped with a Princeton Instrument Micromax camera at 200 $\times$  magnification using Image Pro-plus software.

compared with control showing 3.1% JC-1 monomer positive cells (Figure 5B). The increase in JC-1 monomer is well correlated with dissipation of  $\Delta y_m$ . Valinomycin (10 mM) was used as positive control that showed 27.1% JC-1 monomer positive cells (Figure 5A; quantitative data not shown).

*GSE induces cytochrome c release in cytoplasm in DU145 cells*  
Cytochrome *c* release from mitochondrial intermembranous space into cytosol has been shown to be a key event in the activation of caspase 9 which subsequently initiates a caspase cascade involving caspase 3 and caspase 7 (20). Since GSE-induced the activation of caspase 9, in order to define an upstream event in GSE-induced apoptosis in DU145 cells, we also investigated cytochrome *c* release in cytosolic fraction following GSE treatment of cells. Immunoblot analysis of cytosolic fraction of GSE (150 and 200  $\mu$ g/ml) treated cells showed an increase in the level of cytochrome *c* at 12–72 h treatment duration as compared with control cells (Figure 6, upper panel). 150  $\mu$ g/ml dose of GSE resulted in a peak level of cytochrome *c* at 48 h whereas at 200  $\mu$ g/ml dose of GSE it was at 12 h of treatment. The same membrane was probed with  $\beta$ -actin (Figure 6, lower panel) for loading correction, which did not show any significant change in the protein level of  $\beta$ -actin.

The results showing an increase in the level of cytosolic cytochrome *c* suggested that its release from mitochondria to the cytosol might be an important event in GSE-induced apoptosis, which was further examined and substantiated by

immunohistochemical analysis using cytochrome *c* specific primary antibody and a Alexa 488-conjugated secondary antibody (Figure 6B). Cells were exposed for 12 h with either DMSO (control) or 150  $\mu$ g/ml dose of GSE dissolved in DMSO before immunohistochemical staining. Microscopic examination of cells showed a very less diffused and less intense staining pattern of cytochrome *c* in control cells, which is more indicative of its mitochondrial localization (Figure 6B, control). In GSE-treated cells, a more intense and marked diffuse staining pattern was observed, suggesting that cytochrome *c* has been released from some mitochondria into the cytosol (Figure 6B, GSE). These observations suggest an involvement of cytochrome *c* release from mitochondria as well as a possible disruption of mitochondria in GSE-induced apoptosis in DU145 cells.

## Discussion

The central finding of the present study is that a dietary supplement GSE induces apoptotic death of advanced human prostate carcinoma DU145 cells through caspases activation involving dissipation of mitochondrial membrane potential and cytochrome *c* release from mitochondria into the cytosol. Detailed investigation showed that GSE could induce caspase 3 via more than one mechanisms, in which one involves mitochondrial damage, cytochrome *c* release from mitochondria and caspase 9 activation whereas other(s) is/are independent of caspase 9 activation. These findings present the evidence for a mechanism-based apoptotic effect of GSE on apoptosis resistant prostate carcinoma DU145 cells.

The internally encoded cell suicide program can be induced by several factors, which then converge to a common biochemical caspase pathway leading to execution of apoptosis (21–23). Activation of caspases (a family of cysteine protease) and PARP cleavage are regarded as relevant biomarkers in apoptosis induction (17). Mitochondria, perhaps key regulators of apoptosis, have shown to be involved in integrating different pro-apoptotic pathways via release of cytochrome *c* into the cytosol (18,19). The released cytochrome *c* is complexed with Apaf-1 and pro-caspase 9 in a dATP-dependent manner to form the ‘apoptosome’ from which the release of activated caspase 9 further initiates the activation of caspase cascade leading to biochemical and morphological changes associated with apoptosis (20). Consistent with these reports, GSE increases cleavage of pro-caspases accompanied with an increase in caspase 3-like and caspase 9 protease activities. The increase in caspase 3-like activity by GSE was also accompanied by a PARP cleavage that is one of the substrates of caspase 3-like proteases. GSE-induced activation of caspase 3 is also supported by flow cytometric bead array analysis where a very strong increase in the active caspase 3 level was observed after 48 and 72 h of GSE treatment. Furthermore, the investigation of direct involvement of caspases activation, using caspases inhibitors, showed that up to 90% of GSE-induced apoptosis in DU145 cells is possibly contributed via activation of this pathway. Caspase 3-like caspases seems to be the central caspases in the GSE-activated caspase cascade(s) because blocking of its activity has a similar effect on GSE-induced apoptosis when compared with the use of general caspase inhibitor. Complete inhibition of caspase 9 activity only partially inhibited the GSE-induced apoptosis which suggests that caspase 9 is upstream of caspase 3-like caspases and there may be other mechanism(s) for caspase 3 activation

apart from the cascade mediated through caspase 9 activation. More studies are needed in future to investigate those additional pathways of caspase 3 activation by GSE independent of caspase 9 involvements.

GSE-induced cleavage of pro-caspase 9 and its increased protease activity suggested the possible involvement of cytochrome *c* that is preceded in caspase 9 activation. Our western blot analysis of cytosolic fraction showed that indeed GSE increases cytochrome *c* release from mitochondria to the cytosol. We also observed this effect in immunohistochemical analysis of GSE-treated cells. Fas-mediated apoptosis induction has been shown to induce cytochrome *c* release in human prostatic carcinoma cell lines (24). Since DU145 cells are insensitive to Fas-mediated apoptosis, the effect of GSE on cytochrome *c* release in these cells indicates the involvement of other mechanism(s) independent of Fas-ligand interaction, which is yet to be investigated.

It has been suggested that disruption of  $\Delta y_m$  plays a pivotal role in initiation of apoptotic induction and is also linked to the release of cytochrome *c* from mitochondria to the cytosol (18–20). It is reported that p53-independent proliferation and apoptosis pathways are regulated by  $\Delta y_m$  in human colonic carcinoma cells (25). Since DU145 cells also lack functional p53, we reasoned the involvement of  $\Delta y_m$  in GSE-induced apoptosis in these cells. For this study, we used a mitochondrial membrane potential sensitive cationic JC-1 dye that in the absence of, or at low  $\Delta y_m$ , exists as monomer, emitting at ~525 nm, within the green range of visible light. At higher  $\Delta y_m$ , JC-1 forms 'J-aggregates' that emit at 590 nm, within the orange range of visible light (16). Disruption of  $\Delta y_m$  is an early event in apoptosis induction consistent to GSE induced significant dissipation of  $\Delta y_m$  at 6–12 h of treatment as evidenced by the increase in JC-1 monomer positive cells. These results suggested the involvement of mitochondrial membrane potential damage and induction of cytochrome *c* signaling in GSE-caused apoptotic death of DU145 cells.

Determination of pharmacologically achievable doses is important for any agent to justify its clinical application and to explore molecular mechanisms of the observed effects. Consistent with this notion, it is important to determine whether the doses of GSE used in the present study could be achieved pharmacologically. GSE is a complex mixture containing catechin and epicatechin as single moiety as well as polymers namely, procyanidins, with and without additional substitutions, and some other polyphenolic compounds (26). Accordingly, the quantification of GSE in the biological samples is also a complex issue to address and/or explore. However, in a recent efficacy study of GSE in nude mice PCA xenograft model, we attempted to analyze GSE levels in plasma. For this we developed high performance liquid chromatography profiles for GSE and standard catechin (Sigma), under identical conditions. This approach led us to identify catechin peak in GSE based on retention time, and also its quantification in GSE by area under curve calculation from standard curve derived from catechin. Using this indirect approach, we found that GSE feeding at 100 and 200 mg/kg/day dose for 5 days a week for 7 weeks to nude mice resulted in 52 and 80  $\mu\text{g}$  GSE/ml of the plasma, respectively, which was extrapolated from catechin level (13.8%, w/w) present in GSE (unpublished data). These GSE doses did not show any apparent signs of toxicity to animals in terms of food consumption and body weight gain profile. We also observed that these bioavailable levels of GSE were effective in inhibiting proliferation index

and inducing apoptotic index of prostate carcinoma DU145 tumor xenograft (Singh *et al.*, manuscript under review).

Advanced human prostate carcinoma develops resistance to apoptosis induction to commonly used androgen ablation PCA therapy (4,27). These cancer cells do not respond to tumor necrosis factor  $\alpha$  or Fas-mediated apoptosis that serves as critical target for apoptosis induction by many chemotherapeutic agents (24). Therefore, the control of advanced stages of PCA presents a major challenge in PCA management and therapy. In this regard, efforts are being focused on the search for agents that could induce apoptosis in androgen-independent PCA cells. In the present study, we provide evidence for mechanism-based apoptotic efficacy of GSE against these human PCA DU145 cells. Since GSE is already in human use as a dietary supplement for its several health benefits (28,29), findings of our present study together with those published recently suggest that detailed *in vivo* pre-clinical studies are warranted to evaluate the mechanism-based anticancer (apoptotic) efficacy of GSE against advanced stages of PCA. A positive outcome of such studies might have a clinical application in human PCA patients.

### Acknowledgements

This work was supported in part by AICR grant 00B017 (to CA) and USPHS grants CA83741 and CA64514 (to RA).

### References

- Greenlee,R.T., Hill-Harmon,M.B., Murray,T. and Thun,M. (2001) Cancer statistics, 2001. *CA Cancer J. Clin.*, **51**, 15–36.
- Gioeli,D., Mandell,J.W., Petroni,G.R., Frierson Jr,H.F. and Weber,M.J. (1999) Activation of mitogen-activated protein kinase associated with prostate cancer progression. *Cancer Res.*, **59**, 279–284.
- Agarwal,R. (2000) Cell signaling and regulators of cell cycle as molecular targets for prostate cancer prevention by dietary agents. *Biochem. Pharmacol.*, **60**, 1051–1059.
- Pilat,M.J., Kamradt,J.M. and Pienta,K.J. (1998–99) Hormone resistance in prostate cancer. *Cancer Metastasis Rev.*, **17**, 373–381.
- Raghavan,D., Koczwara,B. and Javle,M. (1997) Evolving strategies of cytotoxic chemotherapy for advanced prostate cancer. *Eur. J. Cancer*, **33**, 566–574.
- Hong,W.K. and Sporn,M.B. (1997) Recent advances in chemoprevention of cancer. *Science*, **278**, 1073–1077.
- Kelloff,G.J., Lieberman,R., Steele,V.E., Boone,C.W., Lubet,R.A., Kopelovitch,L., Malone,W.A., Crowell,J.A. and Sigman,C.C. (1999) Chemoprevention of prostate cancer: concepts and strategies. *Eur. Urol.*, **35**, 342–250.
- Bagchi,D., Garg,A., Krohn,R.L., Bagchi,M., Tran,M.X. and Stohs,S.J. (1997) Oxygen free radical scavenging abilities of vitamin C and E, and a grape seed proanthocyanidin extract in vitro. *Res. Commun. Mol. Pathol. Pharmacol.*, **95**, 179–189.
- Lippert,M.C., McClain,R., Boyd,J.C. and Theodorescu,D. (1999) Alternative medicine use in patients with localized prostate carcinoma treated with curative intent. *Cancer*, **86**, 2642–2648.
- Agarwal,C., Sharma,Y. and Agarwal,R. (2000) Anticarcinogenic effect of a polyphenolic fraction isolated from grape seeds in human prostate carcinoma DU145 cells: modulation of mitogenic signaling and cell cycle regulators and induction of G1 arrest and apoptosis. *Mol. Carcinog.*, **28**, 129–138.
- Agarwal,C., Sharma,Y., Zhao,J. and Agarwal,R. (2000) A polyphenolic fraction from grape seeds causes irreversible growth inhibition of breast carcinoma MDA-MB468 cells by inhibiting mitogen-activated protein kinases activation and inducing G1 arrest and differentiation. *Clin. Cancer Res.*, **6**, 2921–2930.
- Ye,X., Krohn,R.L., Liu,W., *et al.* (1999) The cytotoxic effects of a novel IH636 grape seed proanthocyanidin extract on cultured human cancer cells. *Mol. Cell. Biochem.*, **196**, 99–108.
- Zhao,J., Wang,J., Chen,Y. and Agarwal,R. (1999) Anti-tumor promoting activity of a polyphenolic fraction isolated from grape seeds in mouse

- skin two-stage initiation-promotion protocol, and identification of procyanidin B5-3'-gallate as the most effective antioxidant constituent. *Carcinogenesis*, **20**, 1737–1745.
14. Singletary, K.W. and Meline, B. (2001) Effect of grape seed proanthocyanidins on colon aberrant crypts and breast tumors in a rat dual-organ tumor model. *Nutr. Cancer*, **39**, 252–258.
  15. Nolan, J.P. and Mandy, F.F. (2001) Suspension array technology: new tools for gene and protein analysis. *Cell. Mol. Biol.*, **47**, 1241–1256.
  16. Cossarizza, A., Baccarani-Contri, M., Kalishnikova, G. and Franceschi, C. (1993) A new method for the cytofluorimetric analysis of mitochondrial membrane potential using the J-aggregate forming lipophilic cation 5,5',6,6'-tetrachloro-1,1',3,3'-tetraethylbenzimidazole-carbocyanine iodide (JC-1). *Biochem. Biophys. Res. Commun.*, **30**, 40–45.
  17. Kaufmann, S., Desnoyers, S., Ottaviano, Y., Davidson, N. and Poirier, G. (1993) Specific proteolytic cleavage of poly (ADP-ribose) polymerase: an early marker of chemotherapy-induced apoptosis. *Cancer Res.*, **53**, 3976–3985.
  18. Green, G.R. and Reed, J.C. (1998) Mitochondria and apoptosis. *Science*, **281**, 1309–1312.
  19. Marchetti, P., Castedo, M., Susin, S.A., *et al.* (1996) Mitochondrial permeability transition is central coordinating event of apoptosis. *J. Exp. Med.*, **184**, 1155–1160.
  20. Li, P., Nijhawan, D., Budihardjo, I., Srinivasula, S.M., Ahmed, M., Alnemri, E.S. and Wang, X. (1997) Cytochrome *c* and dATP-dependent formation of Apaf-1/caspase-9 complex initiates an apoptotic protease cascade. *Cell*, **91**, 479–489.
  21. Lowe, S.W. and Lin, A.W. (2000) Apoptosis in cancer. *Carcinogenesis*, **21**, 485–495.
  22. Jiang, C., Wang, Z., Ganther, H. and Lu, J. (2001) Caspases as key executors of methyl selenium-induced apoptosis (anoikis) of DU145 prostate cancer cells. *Cancer Res.*, **61**, 3062–3070.
  23. Marcelli, M., Cunningham, G.R., Walkup, M., *et al.* (1999) Signaling pathway activated during apoptosis of the prostate cancer cell line LNCaP: overexpression of caspase-7 as a new gene therapy strategy for prostate cancer. *Cancer Res.*, **59**, 382–390.
  24. Gewies, A., Rokhlin, O.W. and Cohen, M.B. (2000) Cytochrome *c* is involved in Fas-mediated apoptosis of prostatic carcinoma cell lines. *Cancer Res.*, **60**, 2163–2168.
  25. Heerdt, B.G., Houston, M.A., Anthony, G.M. and Augenlicht, L.H. (1998) Mitochondrial membrane potential ( $Dy_m$ ) in the coordination of p53-independent proliferation and apoptosis pathways in human colonic carcinoma cells. *Cancer Res.*, **58**, 2869–2875.
  26. Escribano-Bailon, M.T., Gutierrez-Fernandez, Y., Rivas-Gonzalo, J.C. and Santos-Buelga, C. (1992) Characterization of procyanidins of *Vitis vinifera* variety Tinta del Paris grape seeds. *J. Agric. Food Chem.*, **40**, 1794–1799.
  27. Koivisto, P., Kolmer, M., Visakorpi, T. and Kallioniemi, O.P. (1998) Androgen receptor gene and hormonal therapy failure of prostate cancer. *Am. J. Pathol.*, **152**, 1–9.
  28. Halpern, M.J., Dahlgren, A.L., Laakso, I., Seppanen-Laakso, T., Dahlgren, J. and McAnulty, P.A. (1998) Red-wine polyphenols and inhibition of platelet aggregation: possible mechanisms, and potential use in health promotion and disease prevention. *J. Int. Med. Res.*, **26**, 171–180.
  29. Bagchi, D., Bagchi, M., Stohs, S. *et al.* (2000) Free radicals and grape seed proanthocyanidin extract: importance in human health and disease prevention. *Toxicology*, **148**, 187–197.

Received May 6, 2002; revised May 29, 2002; accepted July 24, 2002